◆ Human Brain Mapping 35:2643–2651 (2014) ◆

# Multivariate Pattern Analysis of DTI Reveals Differential White Matter in Individuals With Obsessive-Compulsive Disorder

**Fei Li,[1] Xiaoqi Huang,[1] Wanjie Tang,[2] Yanchun Yang,[2]* Bin Li,[2] Graham J. Kemp,[3] Andrea Mechelli,[4] and Qiyong Gong[1]***

[1]*Huaxi MR Research Center (HMRRC), Department of Radiology, West China Hospital of Sichuan University, Chengdu, Sichuan, China*
[2]*Department of Psychiatry, State Key Lab of Biotherapy, West China Hospital of Sichuan University, Chengdu, Sichuan, China*
[3]*Magnetic Resonance and Image Analysis Research Centre (MARIARC), University of Liverpool, Liverpool, United Kingdom*
[4]*Department of Psychosis Studies, Institute of Psychiatry, King's College London, London, United Kingdom*

**Abstract:** Diffusion tensor imaging (DTI) studies have revealed group differences in white matter between patients with obsessive-compulsive disorder (OCD) and healthy controls. However, the results of these studies were based on average differences between the two groups, and therefore had limited clinical applicability. The objective of this study was to investigate whether fractional anisotropy (FA) of white matter can be used to discriminate between patients with OCD and healthy controls at the level of the individual. DTI data were acquired from 28 OCD patients and 28 demographically matched healthy controls, scanned using a 3T MRI system. Differences in FA values of white matter between OCD and healthy controls were examined using a multivariate pattern classification technique known as support vector machine (SVM). SVM applied to FA images correctly identified OCD patients with a sensitivity of 86% and a specificity of 82% resulting in a statistically significant accuracy of 84% ($P \leq 0.001$). This discrimination was based on a distributed network including bilateral prefrontal and temporal regions, inferior fronto-occipital fasciculus, superior fronto-parietal fasciculus, splenium of corpus callosum and left middle cingulum bundle. The present study demonstrates subtle and spatially distributed white matter abnormalities in individuals with OCD, and provides preliminary support for the suggestion that that these could be used to aid the identification of individuals with OCD in clinical practice. *Hum Brain Mapp 35:2643–2651, 2014.* 

**Key words:** obsessive-compulsive disorder; fractional anisotropy; diffusion tensor imaging; support vector machine; multivariate pattern analysis

Xiaoqi Huang and Fei Li contributed equally to this work
Contract grant sponsor: National Natural Science Foundation; Contract grant numbers: 81030027, 81227002, 81220108013, 30700256; Contract grant sponsor: National Key Technologies R&D Program of China; Contract grant numbers: 2012BAI01B03; Contract grant sponsor: Innovative Research Team in University (PCSIRT) of China, Institute of International Education, USA; Contract grant numbers: F510000/G16916411

*Correspondence to: Qiyong Gong or Yanchun Yang; Huaxi MR Research Center (HMRRC), Department of Radiology, West China Hospital of Sichuan University; #37 Guo Xue Xiang, Chengdu, Sichuan, 610041, China. E-mail: qiyonggong@hmrrc.org.cn

Received for publication 12 November 2012; Revised 2 May 2013; Accepted 10 June 2013.
DOI: 10.1002/hbm.22357
Published online 18 September 2013 in Wiley Online Library (wileyonlinelibrary.com).

## INTRODUCTION

Obsessive-compulsive disorder (OCD), a chronic anxiety disorder characterized by repetitive thoughts and behaviors, has a lifetime prevalence of 2–3% [Kessler et al., 2005]. In China, most OCD patients are at the moderate or severe stages [Phillips et al., 2009] and show impaired social and occupational functioning compared with other anxiety or unipolar mood disorders [Torres et al., 2006]. At present there are no laboratory tests for OCD and the diagnosis is made using a standard clinical interview [Abramowitz et al., 2009]. The limited efficacy of traditional selective serotonin reuptake inhibitors in OCD suggests that the serotonin paradigm does not fully explain the neurobiology of this disorder [Macmaster, 2010]. There is therefore an urgent need for a better understanding of the pathophysiology of OCD, which could inform the development of new effective treatments.

In recent years, the success of neuroimaging in defining the neural correlates of OCD has raised hopes that structural or functional biomarkers for this disorder may be found [Linden and Fallgatter, 2009]. In particular, neuroimaging has revealed evidence of the involvement of corticostriatal circuits in OCD, including reduced activation in orbitofrontal cortex [Chamberlain et al., 2008], reduced grey matter density in orbitofrontal and dorsolateral prefrontal cortices, and increased grey matter density in the putamen [Rotge et al., 2009b]. Because these nodes of the corticostriatal circuit are interconnected by white matter tracts, it has been hypothesized that disruption of the connections between frontal cortex and striatum may contribute to the early pathophysiology of OCD [Gruner et al., 2012; Lim and Helpern, 2002]. Consistent with this hypothesis, a recent family-based gene association study has indicated an essential role for white matter abnormalities in the etiology of OCD [Stewart et al., 2007], and neuroimaging studies using diffusion tensor imaging (DTI) have found abnormalities in corpus callosum, frontal and occipital white matter [Li et al., 2011; Menzies et al., 2008b; Szeszko et al., 2005; Yoo et al., 2007]. However, the results of these studies were based on group-level statistics that do not permit evaluation of the discriminative power of these abnormalities at the individual level [Soriano-Mas and Pujol, 2007]; these results have thus had little or no impact on clinical practice.

In recent years, there has been an increasing interest in the use of multivariate pattern analysis (MVPA) for analyzing neuroimaging data [Dosenbach et al.]. MVPA involves the use of powerful pattern classification algorithms to extract spatial and/or temporal patterns from neuroimaging data, and uses this information to categorize individual observations into different categories [Lao et al., 2004]. Compared with traditional mass-univariate approaches, MVPA allows inferences at the level of the individual rather than the group, and as such has greater clinical applicability. In addition, MVPA has the advantage of taking into account interregional correlations, and therefore may be more sensitive to subtle spatially distributed differences [Pereira et al., 2009].

In this study, we used a specific MVPA approach known as support vector machine (SVM). In SVM the classification of individual observations into different categories has two main phases: firstly, an SVM algorithm is trained on a well-characterised sample to establish the hyperplane in a high-dimensional space which best distinguishes the different categories (in this case, patients and controls); secondly, once the optimal hyperplane is developed from the training data, it can be applied to new "testing" data to establish its generalizability [Noble, 2006].

Previous studies using SVM have shown that DTI allows the identification of individual patients with Huntington's disease [Klöppel et al., 2008], mild cognitive impairment [Haller et al., 2010] and Alzheimer's disease [Graña et al., 2011]. To our knowledge, however, no previous study has used SVM to investigate white matter alterations in OCD, and therefore it is unknown whether this would allow the identification of individual OCD patients. Our aims in the present study were two-fold: first, we examined whether the application of SVM to fractional anisotropy (FA) values, as an index of white matter integrity, would allow accurate discrimination between patients with OCD and healthy controls; secondly, we investigated which white matter regions contributed to such discrimination.

## MATERIALS AND METHODS

### Participants

The study was approved by the ethical committee of West China Hospital of Sichuan University, and written informed consent was obtained from all participants. Twenty-eight OCD patients were recruited from the Mental Health Center, West China Hospital, Sichuan University, Chengdu, China. Diagnosis was confirmed using the Structured Clinical Interview for DSM-IV Axis I disorders by two experienced psychiatrists. The patients had no history of previous neurological disorders, psychosurgery, substance abuse or dependence, and there was no evidence of pregnancy or any substantial physical illness from clinical evaluation and medical records. The Yale–Brown Obsessive Compulsive Scale (Y–BOCS) was used to rate the severity of OCD symptoms, whereas the 14-item Hamilton Anxiety Rating Scale (HARS) and 17-item Hamilton Depression Rating Scale (HDRS) were used to rate anxiety and depressive symptoms respectively. Twenty-eight healthy controls matched to the patients for age and sex were recruited from the local community by poster advertisement, and screened using the Structured Clinical Interview for the DSM-Non-Patient edition (SCID-NP) to confirm lifetime absence of psychiatric and neurologic illness, and no history of psychiatric illness in their first-

degree relatives. All participants were reported to have no gross abnormalities on conventional brain MRI images by two experienced radiologists.

### Image Acquisition and Preprocessing

Participants were scanned using a 3T MR imaging system (EXCITE, General Electric) with an 8-channel phased array head coil. Cushions restricted head movements, and participants wore earplugs. DTI images were obtained using a single-shot echo-planar imaging sequence in 50 axial planes with 15 noncollinear diffusion sensitization gradients ($b$ = 1,000 s/mm$^2$), and a reference image with no diffusion weighting ($b_0$ image), using array spatial sensitivity encoding to reduce susceptibility and eddy-current artifacts [Reese et al., 2003]. Imaging parameters were: repetition time/echo time (TR/TE) 12,000/70.8 ms; slice thickness 3 mm (no slice gap); number of excitations 2; matrix 128 × 128; FOV 240 × 240 mm$^2$; voxel size 1.875 × 1.875 × 3 mm$^3$. DTI was performed using axial sections parallel to the anterior–posterior commissural line to cover the entire brain. As an anatomical reference for normalization, high resolution T1-weighted images were acquired using a 3D spoiled gradient recalled (SPGR) sequence (TR/TE, 8.5/3.4 ms; 156 slices with thickness 1 mm; flip angle 12°; matrix 256 × 256; FOV 240 × 240 mm$^2$; voxel size 0.47 × 0.47 × 1 mm$^3$).

DTI-Studio version 3.0.3 (http://cmrm.med.jhmi.edu/) was used to calculate parametric maps of FA value. After images acquisition, the echo planar distortions induced by eddy-current were corrected using an affine transformation algorithm. Image preprocessing was performed with SPM8 software (http://www.fil.ion.ucl.ac.uk/spm) running in MATLAB R2011a. Each subject's $b_0$ image was coregistered with their structural T1 image, and the same coregistration parameters were applied to the FA maps (in the same space as the $b_0$ images). Each T1 image was normalized to the SPM8 T1 template in Montreal Neurological Institute standard space, then the normalization parameters were applied to the coregistered FA images and each voxel was resampled to 2 × 2 × 2 mm$^3$. The normalized FA images were smoothed using an isotropic Gaussian filter (8-mm full width half-maximum).

### Support Vector Machine Analysis

SVM [Vapnik, 1995] was implemented using PROBID (Pattern Recognition of Brain Image Data) software (http://www.brainmap.co.uk/probid.htm) version 1.04. Individual DTI scans were treated as points located in a high dimensional space defined by the FA values in the preprocessed images. A linear decision boundary in this high dimensional space was defined by a "hyperplane" that separated the individual brain scans according to a class label (i.e., patients vs. controls). The optimal hyperplane was computed based on the whole multivariate pattern of FA values across each DTI image. Specifically, a classifier is derived by providing examples of the form $<x, c>$ to find a hyperplane that best separates the input space, where $x$ represents the input data (e.g., FA map) and $c$ is the class label (in this case patients vs. controls). A linear rather than a non-linear kernel SVM was used in order to reduce the risk of overfitting the data and to allow direct extraction of the weight vector as an image (i.e., the SVM discrimination map). The PROBID software allows a linear kernel matrix (measuring similarity between all pairs of brain images) to be precomputed and supplied to the classifier; the similarity measure is simply the dot product between input vectors in feature space. This approach affords a substantial increase in computational efficiency and permits whole-brain classification without requiring explicit dimensionality reduction [Maji et al., 2008] (nonlinear kernels do not increase predictive accuracy [Cox and Savoy, 2003; LaConte et al., 2005]). The linear kernel has just one parameter ($C$) that controls the trade-off between having zero training errors and allowing misclassifications; this parameter was fixed at $C = 1$ for all cases (default value) in accordance with previous neuroimaging studies (e.g. [Mourao-Miranda et al., 2007]). It should be acknowledged, however, that the value of this parameter can have a potentially substantial impact both on the model's prediction accuracy and the reproducibility of its spatial discrimination pattern; this is an outstanding methodological issue which is discussed in detail elsewhere [Rasmussen et al., 2012]. In the present study, to exclude gray matter regions from the SVM analysis, we used a binary white matter mask. A more detailed description of the SVM can be found in the previous reports [Pereira et al., 2009; Vapnik, 1995].

Consistent with previous studies [Gong et al., 2011; Modinos et al., 2012], a "leave-one-out" cross-validation method was used which involved excluding a single subject from each group and training the classifier using the remaining subjects; the subject pair excluded were then used to test the ability of the classifier to reliably distinguish between categories (i.e. patients vs controls). This procedure was repeated for each subject pair in order to assess the overall accuracy of the SVM [Hastie et al., 2001; Pereira et al., 2009]. Statistical significance of the overall classification accuracy was determined by permutation testing [Nichols and Holmes, 2002; Ojala and Garriga, 2010]; this involved repeating the classification procedure 1000 times with a different random permutation of the training group labels; the number of permutations achieving higher sensitivity and specificity than the true labels was used to derive a $P$ value. Statistical significance of classification accuracy was determined by permutation testing. To visualize the multivariate discriminating pattern for FA maps, we show all voxels that have values $\geq$30% of the maximum weight vector value of the discrimination map [Mourao-Miranda et al., 2005].

To examine the degree to which the classification was driven by OCD symptoms rather than other confounds unrelated to OCD, the test margin for each subject was correlated with the level of symptom severity measured by the total Y-BOCS score, the obsessive and compulsive subscale, the HARS and HDRS scores and duration of

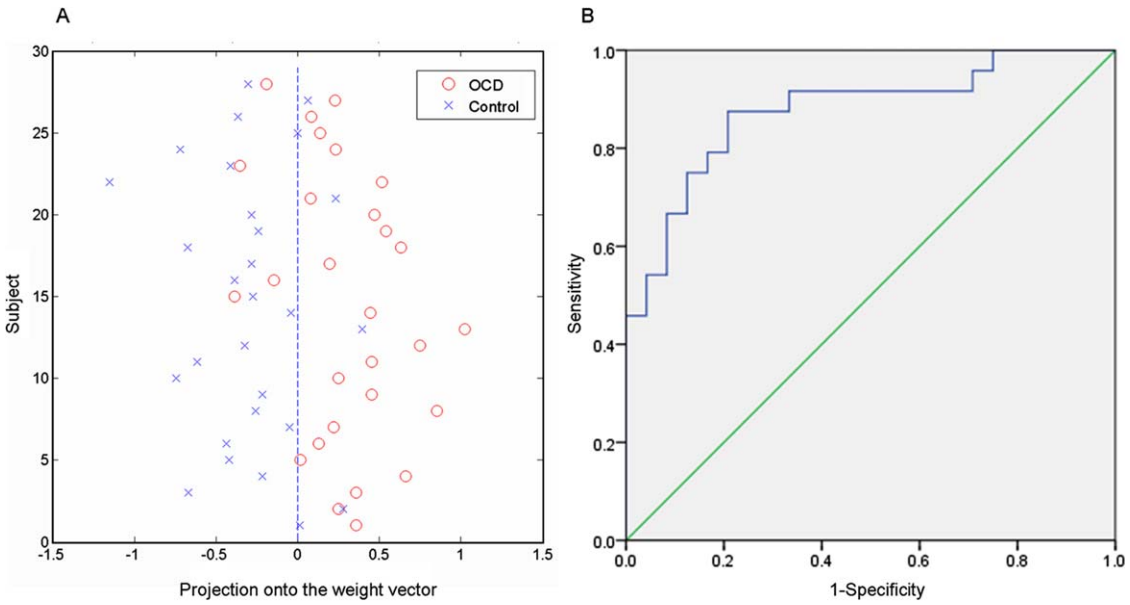


**Figure 1.**

Classification plot (**A**) and Receiver Operating Characteristic (ROC) curve (**B**) for the comparison between 28 OCD patients and 28 healthy controls using FA maps from DTI data, which yielded an accuracy of 84% (86% sensitivity, 82% specificity), statistically significant at $P \leq 0.001$. [Color figure can be viewed in the online issue, which is available at wileyonlinelibrary.com.]

OCD symptoms, respectively (similar approach in previous researches [Ecker et al., 2010a,b]).

## RESULTS

### Demographic and Clinical Characteristics

Between the 28 OCD patients and 28 controls there were no significant differences in sex (10 female, 18 male in both groups), age (mean ± SD 27.8 ± 10.1 range [16–52] vs. 27.6 ± 9.4 [16–46] years, $P = 0.718$, paired $t$-test), and all participants were right-handed. Fifteen patients were drug-naive, while the remaining 13 receiving medication for OCD (4 clomipramine hydrochloride, 3 paroxetine hydrochloride, 3 fluoxetine hydrochloride, 3 sertraline) had been medication-free for ≥ 2 weeks. We classified patients according to the five clinical dimensions defined by Mataix-Cols et al. [1999]. Using these criteria, patients' predominant obsessions/compulsions were as follows: 20 aggressive/checking, 5 contamination/cleaning, 2 symmetry/ordering, 1 sexual/religious; there were no patients with hoarding symptoms. For the 28 OCD patients, the total Y-BOCS was 22.7 ± 3.8 (17–31), corresponding to moderate and severe OCD symptoms, with obsessive and compulsive subscale scores of 16.3 ± 3.7 (10–23) and 6.4 ± 4.9 (0–14) respectively; the estimated duration of OCD symptoms was 6.5 ± 5.5 (1–23) years. The HARS score was 8.0 ± 3.2 (3–19), generally accepted as normal, and the HDRS score was 9.8 ± 2.6 (6–17), indicating mild depression.

### Overall Classifier Performance

Figure 1A shows the result of the SVM classification between 28 OCD and 28 controls based on FA values derived from DTI data. The overall accuracy was 84% (standard error 0.051 and 95% confidence interval 0.777–0.977, with Receiver Operating Characteristic curve shown in Fig. 1B), and was highly significant at $P \leq 0.001$. This overall classification accuracy of the algorithm measures its ability to correctly classify an individual as OCD patient or healthy control. The sensitivity (i.e., the probability that a volunteer with a clinical diagnosis of OCD was correctly assigned to the OCD category) was 86%, and the specificity (i.e., the probability that a healthy control was correctly classified as such) was 82%.

For completeness, we repeated the analysis focusing on the 15 drug-naive OCD patients and 15 age- and sex-matched controls. This yielded a sensitivity of 80% and a specificity of 80%, resulting in an overall accuracy of 80% ($P \leq 0.001$) (Fig. 2).

### Relationship between Test Margin and Level of Symptom Severity

The correlation between the clinical measurements and the distance from the optimal hyperplane (i.e., test margin) was calculated for the OCD group using SPSS 16.0 software (SPSS, Chicago, III). This revealed that the test margin was positively correlated with the total Y-BOCS scores ($r = 0.428$, $P = 0.023$, two tailed): thus individuals with

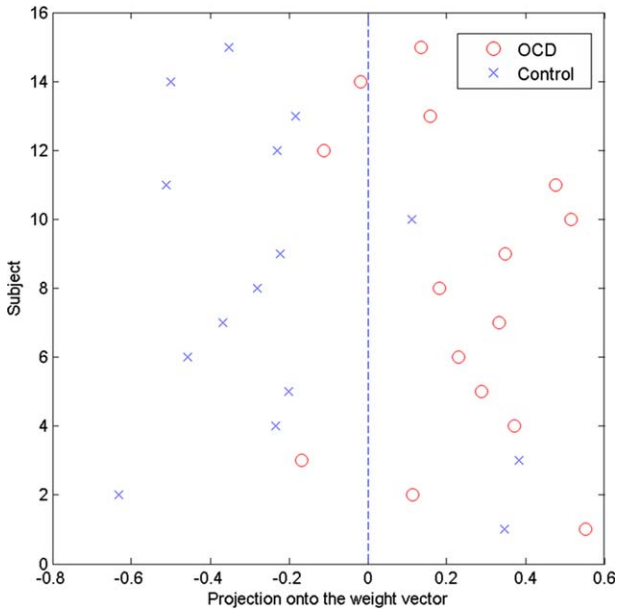


**Figure 2.**

Classification plot for the comparison between 15 drug-naive OCD patients and 15 healthy controls using FA maps from DTI data, which yielded an accuracy of 80% (80% sensitivity, 80% specificity), statistically significant at $P \leq 0.001$. [Color figure can be viewed in the online issue, which is available at wileyonlinelibrary.com.]

higher Y-BOCS scores tended to be further away from the hyperplane while the individuals with a lower level of impairment tended to be nearer the hyperplane. This supports the idea that the classification of these participants on the basis of white matter values was driven by OCD symptoms as measured by Y-BOCS. We did not find significant correlations between the test margin for OCD patients and any of the following measures: obsessive and compulsive subscale, HARS and HDRS scores and duration of OCD symptoms ($P > 0.05$).

### Discrimination Map of OCD Abnormalities

The white matter regions that contributed the most to the discrimination between OCD patients and healthy controls were identified by setting the threshold to $\geq$30% of the maximum weight vector scores, consistent with previous studies (e.g. [Ecker et al., 2010a; Ecker et al., 2010b; Mourao-Miranda et al., 2005]). These regions, shown in Figure 3 and reported in Table 1, included the bilateral prefrontal and temporal white matter, inferior fronto-occipital fasciculus, superior fronto-parietal fasciculus, splenium of corpus callosum, and left middle cingulum bundle. In Figure 3, a positive value in the discrimination map (warm color) indicates that a region contributed to the identification of patients with OCD; this was the case mainly in the left inferior frontal, middle frontal and left cuneus white matter. In contrast, a negative weight (cool color) means that that a region was contributed to the identification of healthy controls; this was the case mainly in the right middle temporal white matter. It should be noted that this discrimination map is a spatial representation of the SVM weight vector, and does not directly quantify the information content of each region. However, the spatial distribution of the weight vector does provide some information about the contribution of different areas to classification [Ecker et al., 2010a] and in this case is suggestive of a distributed pattern of relative deficit or excess of white matter in OCD with respect to healthy controls.

## DISCUSSION

This study demonstrated that patients with OCD can be distinguished from healthy controls using FA images extracted from DTI data with high classification accuracy. This classification was driven by a distributed pattern of white matter alterations which included bilateral prefrontal and temporal white matter, inferior fronto-occipital fasciculus, superior fronto-parietal fasciculus, splenium of corpus callosum, and left middle cingulum bundle. Moreover, in OCD patients the distance from the optimal hyperplane positively correlated with the total Y-BOCS scores, suggesting that the classification of these participants on the basis of white matter values was driven by OCD symptoms.

Multiple white matter microstructural abnormalities in OCD have been reported before [Li et al., 2011; Menzies et al., 2008b; Szeszko et al., 2005; Yoo et al., 2007]. However, previous studies used mass-univariate analyses that tend to detect only a few isolated regions with abnormal FA at group level [Davatzikos, 2004; Soriano-Mas and Pujol, 2007]. Here we used SVM to examine whether the whole-brain pattern of white matter microstructural abnormalities could be used to discriminate between OD patients and healthy controls at the individual level. Unlike mass-univariate analyses, SVM takes inter-regional correlations into account, and provides numerical indicators for group membership without multiple comparison biases [Orrù et al., 2012]. Here a region's discriminative power depends not only on between-group differences in its absolute values, but also on any between-group differences in its structural correlations with other regions; this analytical approach may be particularly suited to the investigation of mental disorders such as OCD in which abnormalities are distributed across the whole brain [Abramowitz et al., 2009; Menzies et al., 2008a]. In the present study discrimination was based not only on frontal regions, cingulum bundle and corpus callosum but also on parts of the occipital and temporal white matter, areas not traditionally implicated in OCD; this demonstrates the ability of SVM to detect subtle and distributed white matter alterations.

Previous neuroimaging studies in OCD have revealed alteration in fronto-striatal circuits [Abramowitz et al., 2009], thought to be important in emotional and

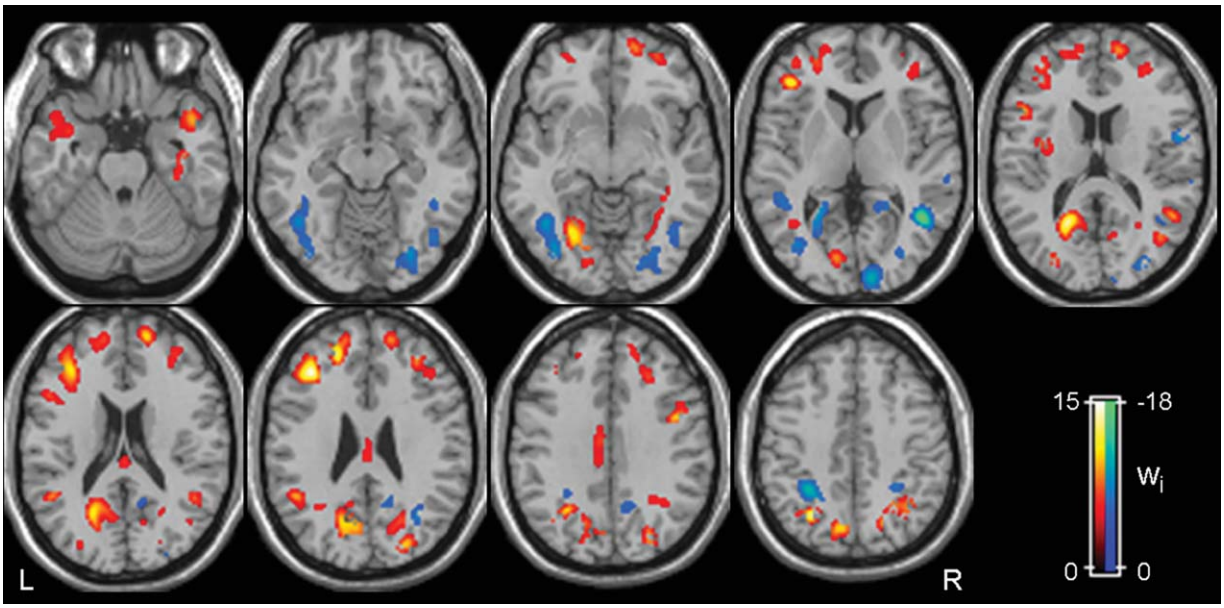


**Figure 3.**

White matter regions contributing to discrimination between OCD and control groups based on FA values. These regions were identified by setting the threshold to $\geq$ 30% of the maximum weight vector scores. Warm color (positive weights) indicates higher parameter values in OCD than healthy controls, while cool color (negative weights) indicates higher parameter values for healthy controls than OCD. The color bar indicates the weight vector value ($w_i$) from the SVM analysis.

motivational aspects of behavior. Alterations within these circuits may explain executive dysfunction, low cognitive-behavioral flexibility and impaired decision-making which are common in OCD [Chamberlain et al., 2008; Menzies et al., 2008a; Rotge et al., 2009a; Saxena et al., 2001]. More specifically, previous DTI studies of OCD have shown increased FA in prefrontal white matter [Li et al., 2011; Menzies et al., 2008b; Yoo et al., 2007; Zarei et al., 2011] that is correlated with symptom severity [Zarei et al., 2011] and is possibly related to increased myelination and neuronal remodeling [Beaulieu, 2002]. These microstructural alterations in frontal white matter may be reversible with citalopram pharmacotherapy, suggesting a functional relationship to the pathophysiology of OCD [Yoo et al., 2007]. In addition, recent genetic studies have proposed an etiologic connection to white matter abnormalities, particularly an association between OCD phenotype and a gene (OLIG2) implicated in oligodendrocyte development [Stewart et al., 2007]. Consistent with these previous DTI studies, we found that prefrontal white matter, especially the left inferior and middle frontal regions, had high discriminative values, supporting the idea that microstructural abnormalities within fronto-striatal circuits are critically affected in OCD.

However, fronto-striatal circuits cannot explain all of the cognitive abnormalities in OCD. For instance, there is evidence of abnormalities in other white matter regions beyond the proverbial fronto-striatal model of OCD, notably the posterior region of the bilateral fronto-occipital and fronto-parietal fasciculi [Menzies et al., 2008a]. The fronto-occipital and fronto-parietal fasciculi connect the frontal lobe to the posterior occipital and parietal cortices respectively [Catani and Thiebaut de Schotten, 2008; Wakana et al., 2004], and previous research has found involvement of the occipital and parietal regions in the clinical phenomenology of OCD, including distressful, intrusive imagery [Garibotto et al., 2010]. Neuropsychological studies of OCD have also reported abnormalities in cognitive processes, such as decision making, that involve a network of regions associated with working memory and visual attention, including the parietal and occipital regions [Ernst et al., 2002; Lawrence et al., 2009]. In addition, neuroimaging studies have reported significant FA differences in occipital and parietal white matter in OCD compared to controls [Gruner et al., 2012; Szeszko et al., 2005; Zarei et al., 2011], which have been related to a pathophysiological hypothesis [Goncalves et al., 2010]. Consistent with these neuropsychological and neuroimaging findings, occipital and parietal white matter contributed to the discrimination between OCD patients and healthy controls in the present study, providing further support for the involvement of these regions in OCD.

Our finding that the bilateral temporal white matter contributed to the identification of OCD patients from healthy

**TABLE 1. White matter regions contributing to discrimination between OCD and control groups. These regions were indentified by setting the threshold to ≥ 30% of the maximum weight vector scores ($w_i$, weight of each cluster centroid, the value of which indicates the relative contribution to the classification).**

| White matter area | Talairach *x* | Talairach *y* | Talairach *z* | $w_i$ |
|---|---|---|---|---|
| OCD > Controls | | | | |
| Frontal | | | | |
| Left superior frontal | −20 | 44 | 26 | 11.20 |
| Right superior frontal | 16 | 56 | 22 | 10.58 |
| Left middle frontal | −36 | 32 | 24 | 14.93 |
| Right middle frontal | 32 | 38 | 24 | 8.35 |
| Left inferior frontal | −42 | 36 | 6 | 11.88 |
| Right precentral | 44 | 2 | 36 | 10.82 |
| Temporal | | | | |
| Left middle temporal | −52 | −38 | −6 | 7.64 |
| Right middle temporal | 48 | −52 | 18 | 8.70 |
| Left temporopolar | −36 | 2 | −20 | 7.53 |
| Right temporopolar | 46 | 10 | −24 | 9.17 |
| Right parahippocampal | 36 | −24 | −22 | 7.41 |
| Left fusiform | −24 | −66 | −8 | 10.17 |
| Right fusiform | 24 | −68 | −10 | 5.41 |
| Occipital | | | | |
| Left middle occipital | −28 | −82 | 14 | 8.70 |
| Right middle occipital | 26 | −82 | 26 | 9.99 |
| Right superior occipital | 22 | −66 | 26 | 7.29 |
| Left cuneus | −20 | −62 | 3 | 13.64 |
| Parietal | | | | |
| Left angular | −28 | −62 | 40 | 10.4 |
| Right inferior parietal lobule | 36 | −56 | 40 | 9.99 |
| Left posterior insula | −34 | −6 | 14 | 6.65 |
| Left middle cingulum bundle | −8 | −14 | 34 | 6.94 |
| Splenium of corpus callosum | 0 | −26 | 22 | 8.35 |
| OCD < Controls | | | | |
| Temporal | | | | |
| Left middle temporal | −46 | −44 | 4 | −9.01 |
| Right middle temporal | 46 | −54 | 6 | −17.88 |
| Left inferior temporal | −44 | −56 | −10 | −10.70 |
| Right inferior temporal | 44 | −42 | −16 | −9.15 |
| Occipital | | | | |
| Left middle occipital | −36 | −72 | 4 | −8.73 |
| Right middle occipital | 30 | −78 | 12 | −11.40 |
| Right superior occipital | 12 | −94 | 6 | −11.83 |
| Left lingual | −24 | −54 | 4 | −12.25 |
| Right lingual | 20 | −48 | 2 | −11.40 |
| Parietal | | | | |
| Left inferior parietal lobule | −30 | −46 | 44 | −12.53 |
| Right inferior parietal lobule | 28 | −46 | 48 | −8.59 |

controls is consistent with other evidence implicating temporal regions in OCD; for instance, patients with temporal lobe epilepsy have a high prevalence of OCD symptoms [Isaacs et al., 2004], and there is a recent report of a patient being diagnosed with OCD following temporal-lobe hemorrhage [Rai et al., 2011]. Previous studies have also reported white matter differences in the temporal regions of OCD patients compared to healthy controls [Yoo et al., 2007], and a significant correlation between FA values in the middle temporal lobe and Y-BOCS [Li et al., 2011].

Although the results of present study are encouraging, there are a number of questions that could not be addressed. We only compared a group of patients with OCD and a group of healthy controls, and therefore it is unclear whether the application of SVM to DTI data would discriminate OCD patients from patients with different disorders. Future studies could address this question by including a third group of patients with an anxiety disorder other than OCD. Furthermore, although all our patients were drug-free for at least 2 weeks before scanning, about half of them had received medication previously. However, we do not believe that medication had a significant influence on the results for two reasons. First, the use of selective serotonin reuptake inhibitors typically leads to a reduction of OCD symptoms as well as a reversible normalization of white matter abnormalities after treatment [Yoo et al., 2007]. Thus, any effect of medication on our results is likely to be expressed in terms of underestimation of the potential of SVM and DTI to identify OCD patients rather than over-estimation. In addition, our results were essentially the same when we repeated the analysis for the drug-naïve subgroup of participants. We also note that, although the OCD group in present study was symptomatically heterogeneous, there were no patients with hoarding symptoms. Given the evidence for differential neural correlates for hoarding and non-hoarding patients with OCD [Saxena et al., 2004], it would be important to replicate our findings in future studies with a larger group of drug-naive OCD patients with different symptoms.

In summary, the present study revealed spatially distributed subtle differential patterns of white matter abnormalities in patients with OCD, and indicated that these abnormalities allow accurate discrimination between OCD

patients and healthy controls at the level of the individual. Although these results are based on a relatively small sample, they provide preliminary support for the potential development of SVM as a diagnostic aid for OCD. Future work could combine white matter information with additional types of neuroimaging data, such as structural and functional MRI, in order to examine whether this leads to higher levels of diagnosis accuracy.

## REFERENCES


Abramowitz JS, Taylor S, McKay D (2009): Obsessive-compulsive disorder. Lancet 374:491–499.

Beaulieu C (2002): The basis of anisotropic water diffusion in the nervous system—A technical review. NMR Biomed 15:435–455.

Catani M, Thiebaut de Schotten M (2008): A diffusion tensor imaging tractography atlas for virtual in vivo dissections. Cortex 44:1105–1132.

Chamberlain SR, Menzies L, Hampshire A, Suckling J, Fineberg NA, del Campo N, Aitken M, Craig K, Owen AM, Bullmore ET (2008): Orbitofrontal dysfunction in patients with obsessive-compulsive disorder and their unaffected relatives. Science 321:421–422.

Cox DD, Savoy RL (2003): Functional magnetic resonance imaging (fMRI) "brain reading": detecting and classifying distributed patterns of fMRI activity in human visual cortex. Neuroimage 19:261–270.

Davatzikos C (2004): Why voxel-based morphometric analysis should be used with great caution when characterizing group differences. Neuroimage 23:17–20.

Dosenbach NUF, Nardos B, Cohen AL, Fair DA, Power JD, Church JA, Nelson SM, Wig GS, Vogel AC, Lessov-Schlaggar CN (2010): Prediction of individual brain maturity using fMRI. Science 329:1358–1361.

Ecker C, Marquand A, Mour o-Miranda J, Johnston P, Daly EM, Brammer MJ, Maltezos S, Murphy CM, Robertson D, Williams SC (2010a): Describing the brain in autism in five dimensions—Magnetic resonance imaging-assisted diagnosis of autism spectrum disorder using a multiparameter classification approach. J Neurosci 30:10612–10623.

Ecker C, Rocha-Rego V, Johnston P, Mourao-Miranda J, Marquand A, Daly EM, Brammer MJ, Murphy C, Murphy DG (2010b): Investigating the predictive value of whole-brain structural MR scans in autism: A pattern classification approach. Neuroimage 49:44–56.

Ernst M, Bolla K, Mouratidis M, Contoreggi C, Matochik JA, Kurian V, Cadet JL, Kimes AS, London ED (2002): Decision-making in a Risk-taking Task: A PET Study. Neuropsychopharmacology 26:682–691.

Garibotto V, Scifo P, Gorini A, Alonso CR, Brambati S, Bellodi L, Perani D (2010): Disorganization of anatomical connectivity in obsessive compulsive disorder: A multi-parameter diffusion tensor imaging study in a subpopulation of patients. Neurobiol Dis 37:468–476.

Goncalves OF, Marques TR, Lori NF, Sampaio A, Branco MC (2010): Obsessive-compulsive disorder as a visual processing impairment. Med Hypotheses 74:107–109.

Gong Q, Wu Q, Scarpazza C, Lui S, Jia Z, Marquand A, Huang X, McGuire P, Mechelli A (2011): Prognostic prediction of therapeutic response in depression using high-field MR imaging. Neuroimage 55:1497–1503.

Graña M, Termenon M, Savio A, Gonzalez-Pinto A, Echeveste J, Pérez JM, Besga A (2011): Computer aided diagnosis system for Alzheimer disease using brain diffusion tensor imaging features selected by Pearson's correlation. Neurosci Lett 502:225–229.

Gruner P, Vo A, Ikuta T, Mahon K, Peters BD, Malhotra AK, Ulug AM, Szeszko PR (2012): White matter abnormalities in pediatric obsessive-compulsive disorder. Neuropsychopharmacology 37:2730–2739.

Haller S, Nguyen D, Rodriguez C, Emch J, Gold G, Bartsch A, Lovblad KO, Giannakopoulos P (2010): Individual prediction of cognitive decline in mild cognitive impairment using support vector machine-based analysis of diffusion tensor imaging data. J Alzheimers Dis 22:315–327.

Hastie T, Tibshirani R, Friedman J (2001): The Elements of Statistical Learning: Data Mining, Inference, and Prediction. New York, NY: Springer-Verlag.

Isaacs KL, Philbeck JW, Barr WB, Devinsky O, Alper K (2004): Obsessive-compulsive symptoms in patients with temporal lobe epilepsy. Epilepsy Behav 5:569–574.

Kessler RC, Berglund P, Demler O, Jin R, Merikangas KR, Walters EE (2005): Lifetime prevalence and age-of-onset distributions of DSM-IV disorders in the National Comorbidity Survey Replication. Arch Gen Psychiatry 62:593–602.

Klöppel S, Draganski B, Golding CV, Chu C, Nagy Z, Cook PA, Hicks SL, Kennard C, Alexander DC, Parker GJM (2008): White matter connections reflect changes in voluntary-guided saccades in pre-symptomatic Huntington's disease. Brain 131: 196–204.

LaConte S, Strother S, Cherkassky V, Anderson J, Hu X (2005): Support vector machines for temporal classification of block design fMRI data. NeuroImage 26:317–329.

Lao Z, Shen D, Xue Z, Karacali B, Resnick SM, Davatzikos C (2004): Morphological classification of brains via high-dimensional shape transformations and machine learning methods. Neuroimage 21:46–57.

Lawrence NS, Jollant F, O'Daly O, Zelaya F, Phillips ML (2009): Distinct roles of prefrontal cortical subregions in the Iowa Gambling Task. Cerebral Cortex 19:1134–1143.

Li F, Huang X, Yang Y, Li B, Wu Q, Zhang T, Lui S, Kemp GJ, Gong Q (2011): Microstructural brain abnormalities in patients with obsessive-compulsive disorder: Diffusion-tensor MR imaging study at 3.0 T. Radiology 260:216–223.

Lim KO, Helpern JA (2002): Neuropsychiatric applications of DTI—A review. NMR Biomed 15:587–593.

Linden DE, Fallgatter AJ (2009): Neuroimaging in psychiatry: From bench to bedside. Front Hum Neurosci 3:49.

Macmaster FP (2010): Translational neuroimaging research in pediatric obsessive-compulsive disorder. Dialogues Clin Neurosci 12:165–174.

Maji S, Berg AC, Malik J. (Classification using intersection kernel support vector machines is efficient). In; 2008. IEEE Computer Vision and Pattern Recognition. p 1–8.

Mataix-Cols D, Rauch SL, Manzo PA, Jenike MA, Baer L (1999): Use of factor-analyzed symptom dimensions to predict outcome with serotonin reuptake inhibitors and placebo in the treatment of obsessive-compulsive disorder. Am J Psychiatry 156:1409–1416.

Menzies L, Chamberlain SR, Laird AR, Thelen SM, Sahakian BJ, Bullmore ET (2008a): Integrating evidence from neuroimaging and neuropsychological studies of obsessive-compulsive disorder: The orbitofronto-striatal model revisited. Neurosci Biobehav Rev 32:525–549.

Menzies L, Williams GB, Chamberlain SR, Ooi C, Fineberg N, Suckling J, Sahakian BJ, Robbins TW, Bullmore ET (2008b): White matter abnormalities in patients with obsessive-compulsive disorder and their first-degree relatives. Am J Psychiatry 165:1308–1315.

Modinos G, Pettersson-Yeo W, Allen P, McGuire PK, Aleman A, Mechelli A (2012): Multivariate pattern classification reveals differential brain activation during emotional processing in individuals with psychosis proneness. Neuroimage 59:3033–3041.

Mourao-Miranda J, Bokde AL, Born C, Hampel H, Stetter M (2005): Classifying brain states and determining the discriminating activation patterns: Support Vector Machine on functional MRI data. Neuroimage 28:980–995.

Mourao-Miranda J, Friston KJ, Brammer M (2007): Dynamic discrimination analysis: A spatial-temporal SVM. Neuroimage 36:88–99.

Nichols TE, Holmes AP (2002): Nonparametric permutation tests for functional neuroimaging: A primer with examples. Human Brain Mapp 15:1–25.

Noble WS (2006): What is a support vector machine? Nat Biotechnol 24:1565–1567.

Ojala M, Garriga GC (2010): Permutation tests for studying classifier performance. J Machine Learning Res 11:1833–1863.

Orrù G, Pettersson-Yeo W, Marquand AF, Sartori G, Mechelli A (2012): Using Support Vector Machine to identify imaging biomarkers of neurological and psychiatric disease: A critical review. Neurosci Biobehav Rev 36:1140–1152.

Pereira F, Mitchell T, Botvinick M (2009): Machine learning classifiers and fMRI: A tutorial overview. Neuroimage 45:S199–S209.

Phillips MR, Zhang J, Shi Q, Song Z, Ding Z, Pang S, Li X, Zhang Y, Wang Z (2009): Prevalence, treatment, and associated disability of mental disorders in four provinces in China during 2001-05: An epidemiological survey. Lancet 373:2041–2053.

Rai A, Chopra A, Das P (2011): Obsessive-compulsive disorder after right temporal-lobe hemorrhage. J Neuropsychiatry Clin Neurosci 23:E13.

Rasmussen PM, Hansen LK, Madsen KH, Churchill NW, Strother SC (2012): Model sparsity and brain pattern interpretation of classification models in neuroimaging. Pattern Recognition 45: 2085–2100.

Reese TG, Heid O, Weisskoff RM, Wedeen VJ (2003): Reduction of eddy-current-induced distortion in diffusion MRI using a twice-refocused spin echo. Magn Reson Med 49:177–182.

Rotge JY, Guehl D, Dilharreguy B, Tignol J, Bioulac B, Allard M, Burbaud P, Aouizerate B (2009a): Meta-analysis of brain volume changes in obsessive-compulsive disorder. Biol Psychiatry 65:75–83.

Rotge JY, Langbour N, Guehl D, Bioulac B, Jaafari N, Allard M, Aouizerate B, Burbaud P (2009b): Gray matter alterations in obsessive–compulsive disorder: An anatomic likelihood estimation meta-analysis. Neuropsychopharmacology 35:686–691.

Saxena S, Bota RG, Brody AL (2001): Brain-behavior relationships in obsessive-compulsive disorder. Semin Clin Neuropsychiatry 6:82–101.

Saxena S, Brody AL, Maidment KM, Smith EC, Zohrabi N, Katz E, Baker SK, Baxter LR Jr. (2004): Cerebral glucose metabolism in obsessive-compulsive hoarding. Am J Psychiatry 161:1038–1048.

Soriano-Mas C, Pujol J (2007): Identifying patients with obsessive-compulsive disorder using whole-brain anatomy. Neuroimage 35:1028–1037.

Stewart SE, Platko J, Fagerness J, Bims J, Jenike E, Smaller JW, Perlis R, Leboyer M, Delorme R, Chabane N (2007): A genetic family-based association study of OLIG2 in obsessive-compulsive disorder. Arch Gen psychiatry 64:209–215.

Szeszko PR, Ardekani BA, Ashtari M, Malhotra AK, Robinson DG, Bilder RM, Lim KO (2005): White matter abnormalities in obsessive-compulsive disorder: A diffusion tensor imaging study. Arch Gen Psychiatry 62:782–790.

Torres AR, Prince MJ, Bebbington PE, Bhugra D, Brugha TS, Farrell M, Jenkins R, Lewis G, Meltzer H, Singleton N (2006): Obsessive-compulsive disorder: Prevalence, comorbidity, impact, and help-seeking in the British National Psychiatric Morbidity Survey of 2000. Am J Psychiatry 163:1978–1985.

Vapnik VN (1995): The nature of statistical learning theory. Springer-Verlag, New York.

Wakana S, Jiang H, Nagae-Poetscher LM, van Zijl PC, Mori S (2004): Fiber tract-based atlas of human white matter anatomy. Radiology 230:77–87.

Yoo SY, Jang JH, Shin YW, Kim DJ, Park HJ, Moon WJ, Chung EC, Lee JM, Kim IY, Kim SI, Kwon JS (2007): White matter abnormalities in drug-naive patients with obsessive-compulsive disorder: A diffusion tensor study before and after citalopram treatment. Acta Psychiatr Scand 116:211–219.

Zarei M, Mataix-Cols D, Heyman I, Hough M, Doherty J, Burge L, Winmill L, Nijhawan S, Matthews PM, James A (2011): Changes in gray matter volume and white matter microstructure in adolescents with obsessive-compulsive disorder. Biol Psychiatry 70:1083–1090.